

The functional and structural effects of an amphipathic pH responsive biopolymer: a comprehensive study in osteosarcoma cells

Mercado S. A., Slater N. K. H. *

Department of Chemical Engineering and Biotechnology, University of Cambridge, Pembroke Street, Cambridge CB2 3RA, United Kingdom

*Corresponding author. Tel.: +44 (0) 1223 762953; Fax: +44 (0) 1223 334796

Email address: nkhs2@cam.ac.uk (N. Slater)

Abstract

The use of amphipathic pH-responsive polymers to transport sugars across cell membranes has been shown to improve the cryopreservation of mammalian cells. However, the effect of these polymers on cell viability and morphology has not yet been thoroughly analysed. In this study, the objective was to investigate the functional and structural effects of an amphipathic polymer, PP-50, upon an osteosarcoma cell line (SAOS-2). Cellular growth curves confirmed similar doubling times in PP-50 treated cells and untreated cells. PP-50 concentrations (10-2000 µg/ml) were well tolerated by cells after 2, 24 and 48 hours of incubation, as measured by mitochondrial enzyme activity and lactate dehydrogenase release. Analysis by flow cytometry demonstrated that PP-50 did not induce any additional apoptosis or necrosis in polymer treated cells compared to untreated cells. Phase contrast, confocal and transmission electron microscopy analysis of PP-50 treated cells revealed no signs of morphological changes, with cells maintaining their nucleus size and membrane integrity after treatment. PP-50 was shown to have no negative cellular effects, which is a critical characteristic of polymers towards use in cryopreservation and biomedical applications. In addition, the methodology and protocols established in this work provided a robust and comprehensive analysis of PP-50's cellular effects, thus making them well suited for determining these effects in mammalian cells exposed to other polymers intended for biological applications.

Key words

Amphipathic polymer, cytotoxicity, membrane permeabilisation, cryopreservation, drug delivery

1. Introduction

The ability of biopolymers to act as carrier systems makes them attractive for biological applications [1,2]. Biopolymers are able to transport a variety of molecules, such as successful cancer therapy candidates and proteins, across mammalian cell membranes, acting as permeabilising agents and improving the pharmacological and therapeutic properties of drugs [3,4]. The role of biopolymers in the advancement of drug delivery systems (DDS) has been well documented, with polymers providing controlled release of therapeutic agents over long periods, cyclic dosage, and adjustable release of both hydrophilic and hydrophobic drugs [5,6]. However, little attention has been given in the literature to the effect of biopolymer delivery systems on cell physiology [4,7].

In addition to their role as DDS, polymers have been shown to be effective in the cryopreservation of mammalian cells [8,9]. Currently, cryopreservation of cell lines is a technically demanding process leading to recurrent failures related to poor revival rates and atypical cell properties. Cryopreservation techniques must be improved to overcome difficulties in the transportation and prolonged storage of mammalian and stem cells, as these issues have hindered their use in clinical studies and industrial applications [10–12].

To survive long-term storage at low temperatures, cells typically require cryoprotective agents (CPAs), such as dimethyl sulfoxide (Me_2SO) or glycerol [13–15]. However, successful cryopreservation of mammalian cells requires high concentrations of CPAs and their toxicity has been recognised as a critical barrier to further advancement of the field [13,16].

Sugars are key non-toxic components in a large number of cryopreservation protocols. They help in the dehydration of cells by increasing osmolarity, in addition to preserving structural integrity. They also function as an osmotic buffer, reducing osmotic shock by decreasing the rate and amount of cell swelling [17,18]. However, sugar transport across animal cell membranes is restricted to monosaccharides since disaccharides do not readily diffuse across the plasma membrane [19]. This is a major challenge when high concentrations of disaccharides such as trehalose are needed within cells for viable cryopreservation [13,20].

To overcome this obstacle, different approaches have been developed to increase the levels of intracellular disaccharides, such as the use of ATP receptor channels or engineered membrane pores [20–22]. Disadvantages of these alternatives include the induction of cell death by either necrosis or apoptosis, amongst others [23].

One effective method to induce disaccharide transport into cells involves the use of amphipathic biodegradable pH-responsive polymers due to their ability to permeate cell membranes [9,24]. These polymers have been developed to mimic the membrane permeabilising activity of viral and bacterial peptides [25]. Typically, they undergo a conformational change from extended charged chains to aggregated hydrophobic structures as the environmental pH drops below their pKa, thus interacting with the hydrophobic interior of phospholipid bilayers. This facilitates increased membrane permeability by pore formation or by increasing membrane solubilisation [26,27].

Recently, research focused on the cryopreservation of human red blood cells and osteosarcoma cells has shown an increase in phospholipid bilayer permeability to trehalose when using the biopolymer PP-50, a polymer consisting of poly(L-lysine iso-phthalamide) grafted with the hydrophobic amino acid L-phenylalanine. This has successfully led to an increase in post-thaw viabilities of cryopreserved mammalian cells [8,28].

Despite its successful use in cryopreservation, the effect of PP-50 on cell viability, membrane integrity and cell morphology has not been studied in depth in previous works. In this study, the effect of PP-50 on these characteristics was evaluated in osteosarcoma cells, a model for adherent cells, to provide key information regarding this amphipathic biopolymer towards use in cryopreservation and other clinical applications. In addition, the methodology and protocols established in this work provided a robust and comprehensive analysis of PP-50's cellular effects, thus making them well suited for determining these effects in mammalian cells exposed to other polymers intended for biological applications.

2. Materials and methods

2.1. Materials

The SAOS-2 cells were obtained from the European Collection of Cell Cultures. Dulbecco's modified Eagle's medium (DMEM), foetal bovine serum (FBS), L-glutamine, penicillin, streptomycin and trypan blue were purchased from Invitrogen (UK). Phosphate-Buffered Saline (PBS) and trypsin-EDTA were purchased from Life Technologies™ (UK). The CellTiter 96® Aqueous One Solution Cell Proliferation Assay (MTS) was obtained from Promega (UK). The Annexin V-FITC Apoptosis Detection Kit was obtained from BD Biosciences (UK). The Lactate Dehydrogenase (LDH) Activity Assay Kit, calcein, propidium

iodide (PI) and Hoechst H33342 were obtained from Sigma-Aldrich (UK). All chemicals and biochemicals used were of analytical grade.

2.2. PP-50 synthesis and characterisation

The synthesis and characterisation of the PP-50 polymer were as previously described by Lynch *et al.* [28]. PP-50 consists of a poly(L-lysine iso-phthalamide) backbone grafted with L-phenylalanine at a degree of grafting of 46.2% (Mn = 23.0 kDa)

2.3. Cell culture

SAOS-2 osteosarcoma cells were cultured in DMEM with FBS (10% v/v), L-glutamine (2 mM), penicillin (100 IU/ml), and streptomycin (100 µg/ml) in 75 cm² flasks supplied by Corning (UK). Cells were incubated in a 37°C incubator with 5% of CO₂. At 70% confluence, cells were washed twice with PBS, then subcultured with trypsin (0.05% w/v) and EDTA (0.02% w/v) and subsequently replated for further expansion or cytotoxicity studies.

2.4. Cellular growth curves

Cells were passaged into 12-well plates (0.2 x 10⁶ cell/well) and grown for 24 hrs. Cells were then incubated with PP-50 (25 and 250 µg/ml) for 120 hrs. Control cells were incubated in growth media without PP-50. Cell density and viability were determined every 24 hrs by the trypan blue (TB) exclusion method using a cell counter [29]. Cells negative for TB were considered live and those stained blue were considered dead. The doubling times (t_d) were calculated using Eq. (1), where t_1 and t_2 represent the time at time-points 1 and 2, respectively, and $N(t_1)$ and $N(t_2)$ represent the number of cells at time-points 1 and 2, respectively.

$$t = (t_2 - t_1) \frac{\ln(2)}{\ln\left(\frac{N_{t_2}}{N_{t_1}}\right)} \quad (1)$$

2.5. Cytotoxicity tests

The cytotoxicity of the polymer PP-50 was evaluated using colorimetric MTS and LDH tests. A range of concentrations between 10 and 2,000 µg/ml of PP-50 were tested after 2, 24 and 48 hour incubations. Different incubation times were used to assess cell viability by measuring cell growth in the presence of PP-50 [20,30].

2.5.1. MTS test

Cells were passaged into 96-well plates (5×10^3 cells/well) and grown for 24 hours. Cells were then washed with PBS and incubated with PP-50 (10 to 2,000 $\mu\text{g/ml}$) for 2, 24 and 48 hours. Viable cells were determined using the CellTiter 96® AQueous One Solution Cell Proliferation Assay according to the manufacturer's instructions. Absorbance was measured at 490 nm using a 96-well plate reader (BMG Labtech, UK) and corrected by subtraction of background absorbance.

2.5.2. LDH test

Cells were passaged into 96-well plates (5×10^3 cells/well) and grown for 24 hours. After 2, 24 and 48 hours of incubation with PP-50, 50 μl of the cell growth media were removed from each sample and assayed for lactate dehydrogenase using the Lactate Dehydrogenase Activity Assay Kit, according to the manufacturer's instructions. Media from lysis buffer (Triton-X 0.2% v/v) were used to determine maximal release values. Absorbance was measured at 450 nm using a 96-well plate reader and corrected by subtraction of background absorbance.

2.6. Apoptosis assessment

2.6.1. Flow cytometry

For early apoptosis quantification, cells were incubated with 250 $\mu\text{g/ml}$ of PP-50 and then analysed using the Annexin-V-FITC/propidium iodide Assay Kit according to the manufacturer's instructions, using a FACScan flow cytometer (Becton Dickinson, USA). A staurosporine treatment (5 μM for 2 hours) was used as a positive control for apoptotic cells. Data were acquired using Cellquest software and analysed using the Beckman Coulter Summit software.

2.7. Cell morphology

2.7.1. Phase contrast microscopy

Cells were passaged into 6 well plates (0.5×10^6 cells/well) and grown for 24 hours. After exposure to 250 $\mu\text{g/ml}$ of PP-50 for 2 and 24 hours, cells were examined by a contrast light microscope. Control cells were incubated in growth media without PP-50.

2.7.2. Confocal microscopy

Cells were assessed using 2 mM calcein and 5 $\mu\text{g/ml}$ propidium iodide (PI) stains in the absence and presence of the polymer. In addition, the permeable dye Hoechst 33342 (5 $\mu\text{g/ml}$), was used to evaluate the nuclear morphology of cells. Cells were placed on 1.8 cm^2 chambered cell culture cover glasses (Nunc, UK) at a density of 5×10^4 cells/well and imaged using a TCS SP5 inverted laser scanning microscope (Leica, Germany) after 24 hour incubation. A positive control for PI staining was prepared using fixation with paraformaldehyde solution (4% w/v) for 15 minutes.

2.7.3. Transmission electron microscopy

The cell morphology of SAOS-2 cells was evaluated using transmission electron microscopy. Cells were incubated in the absence and presence of PP-50 for 2 and 24 hours and then washed twice with saline buffer (0.155 M NaCl). Subsequently, cells were fixed in 4% glutaraldehyde in 0.1 M HEPES buffer at pH 7.4 for 12 hours at 4° C. They were rinsed in 0.1 M HEPES buffer five times and then treated with 1% osmium ferricyanide at room temperature for 2 hours. Next, they were rinsed in deionised water five times and treated with 2% uranyl acetate in 0.05 M maleate buffer at pH 5.5 for 2 hours at room temperature. They were again rinsed in deionised water and dehydrated in an ascending series of ethanol solutions from 70% to 100%. This was followed by treatment with 2 changes of dry acetonitrile and infiltration with Quetol epoxy resin. Images were examined under a transmission electron microscope (Tecnai G2, FEI Company, USA) operated at 120 kV using an AMT XR60B digital camera running Deben software.

2.8 Statistical analysis

All measurements were carried out by triplicate in three different replicates. The flow cytometry results were analysed using a one-way ANOVA followed by a Tukey's test for multiple comparisons. The tests were analysed using GraphPad Prism (GraphPad Software, US). The difference was considered statistically significant when $p < 0.05$.

3. Results

3.1 Cellular growth curves

Cell growth in the presence of PP-50 was measured using the trypan blue exclusion method over 120 hrs (Fig. 1). As seen in Fig. 1, cell density increased in an exponential fashion for the control and cells treated with 25 µg/ml of PP-50. Cells treated with 250 µg/ml of PP-50 showed a decrease in cell density when compared to control. The doubling times were 27.7 ± 1.58 hrs, 28 ± 1.76 hrs and 32 ± 0.16 hrs for the control, 25 µg/ml and 250 µg/ml of PP50, respectively. Cell viabilities in all conditions tested remained higher than 90% during the entire incubation period.

3.2 Cytotoxicity of PP-50

3.2.1. Metabolic activity

The effect on metabolic activity of cells incubated with PP-50 was investigated using the MTS assay (Fig. 2). The cytotoxicity was examined as a function of the polymer concentration and incubation time. PP-50 concentrations ranging from 10 to 2,000 µg/ml were not cytotoxic and were well tolerated by the cells after 2, 24 and 48 hour incubations. PP-50 only showed a marginal decrease in metabolic activity at 1,500 and 2,000 µg/ml after 48 hours of incubation.

3.2.2. LDH assay

The effect on membrane integrity in osteosarcoma cells was studied using the LDH assay (Fig. 3). Media samples from cells treated with PP-50 for 2, 24 and 48 hours were assayed for lactate dehydrogenase. As seen in Fig. 3, PP-50 did not increase the release of LDH into the media of PP-50 treated cells compared to the untreated control. Reduced LDH release was observed in the entire range of PP-50 concentrations, with levels of less than 20% at concentrations up to 2,000 µg/ml of PP-50, similar to the untreated cells.

3.3. Assessment of apoptosis

3.3.1. Flow cytometry

The induction of apoptosis was assessed by incubating cells with 250 µg/ml of PP-50 for 2 and 24 hours (Fig. 4). Apoptosis and necrosis were observed using the Annexin V-FITC/PI

Kit. As shown in Fig. 4, there was a significant decrease ($p < 0.05$) in apoptotic cells after 2 and 24 hours of incubation with PP-50 when compared to untreated cells. The percentage of apoptotic cells after 2 and 24 hours of incubation in the control group was $20\% \pm 1.4\%$ and $13\% \pm 0.5\%$, respectively, whereas cells treated with PP-50 had apoptotic percentages of $10\% \pm 0.4\%$ and $9\% \pm 0.5$, respectively. Polymer treated cells after 2 and 24 hours of incubation also showed a significant decrease ($p < 0.05$) of 64% and 67%, respectively, in apoptotic cells when compared to cells treated with staurosporine.

In addition, there was also a significant decrease ($p < 0.05$) in necrotic cells in PP-50 treated cells after 24 hours of incubation when compared to the control. The percentage of necrotic cells after 24 hours of incubation in the control group was $5\% \pm 0.4\%$, whereas cells treated with PP-50 had a necrotic percentage of $2\% \pm 0.13\%$.

3.4. Cell Morphology

3.4.1. Phase contrast microscopy

After exposure to 250 $\mu\text{g/ml}$ of PP-50 for 2 and 24 hours, cell morphology was examined by phase contrast microscopy (Fig. 5). Clearly visible cytoskeletons were observed in both control and PP-50 treated cells, with the majority of cells attached to the surface. There was a marginal detachment of cells from the well in PP-50 treated cells. Additionally, control and PP-50 treated cells showed normal morphology when compared to staurosporine treated cells, a well-known apoptosis inducer.

3.4.2. Confocal microscopy

The cell morphology after incubation with 200 $\mu\text{g/ml}$ of PP-50 for 24 hours was also evaluated by calcein, propidium iodide and Hoechst 33342 fluorescence assay using confocal microscopy (Fig. 6). As shown in Fig. 6, there was no staining with propidium iodide either for untreated or PP-50 treated cells. Cells incubated in the presence of PP-50 also displayed normal nuclei features, shown by the staining with Hoechst H33342. Calcein staining was seen only in the membrane of control cells, whereas in PP-50 treated cells, the staining was stronger and seen inside the cells. Similar results were also obtained for 2 hours of incubation with PP-50 (data not shown).

3.4.3. Transmission electron microscopy

Transmission electron microscopy was utilised to further investigate morphological changes in cells incubated with PP-50 (Fig. 7). The ultrastructural features in SAOS-2 cells revealed regular nuclear membrane, intact nucleoli, homogeneous chromatin, and visible microvilli in both control and PP-50 treated cells. No morphological signs of apoptosis were observed either in the control or PP-50 treated cells.

4. Discussion

Previous studies have reported different methodologies to assess polymer cytotoxicity in mammalian cells [4,7]. However, a comprehensive study was needed to accurately determine cell viability, i.e., the parallel investigation of cell growth, metabolic activity, membrane integrity, and cell morphology.

In this study, the cellular effect of PP-50 was tested in SAOS-2 cells. Analysis by trypan blue exclusion, MTS, LDH, and Annexin V-FITC/PI assays, as well as phase contrast, transmission electron and confocal microscopy, all showed that incubations with PP-50 did not increase cell cytotoxicity when compared to controls at the concentrations tested.

Cell growth in the presence of PP-50 was studied using the trypan blue exclusion method (Fig. 1). Similar growth curves and viabilities were obtained with control cells and with cells treated with 25 µg/ml of PP-50. Although cell density was affected when incubating with 250 µg/ml of PP-50, doubling time was not altered significantly (a 15% increase compared to control). This reduction in cell density can be explained partially by (1) cell detachment occurring at higher concentrations of PP-50 after long incubations and (2) the subsequent loss of cells in the washing steps prior to cell counting. Hence, detached cells are not taken into account for the calculation of cell density. However, PP-50 is typically used for biological applications in much lower concentrations with shorter incubation times. Previous studies have proven PP-50 to have a permeabilising effect on cell membranes when incubated at a low concentration of 25 µg/ml for less than 24 hours [8,28].

Another factor possibly involved in this decrease in cell viability is the use of the trypan blue staining method. Despite the fact that it is widely used for measuring cell density, this method has several inherent disadvantages. It has been described in numerous studies as highly subjective and possessing significant accuracy errors [29,31].

Metabolic activity of SAOS-2 cells was investigated using the MTS assay, a colorimetric method that measures the activity of cell cytoplasmic esterases (Fig. 2). PP-50

concentrations ranging from 10 to 2000 µg/ml showed no toxic effect and no significant decrease in metabolic activity compared to untreated cells. These results are in agreement with previous studies [8].

Membrane integrity was evaluated using the LDH assay (Fig. 3). LDH is a soluble cytosolic enzyme that is released into the culture medium following the loss of membrane integrity. Therefore, LDH activity can be used to determine loss of plasma membrane integrity due to biochemical perturbations [32,33]. After treatment with PP-50, the cell membranes remained intact, as shown by low LDH values below 20%. Cell exposure to PP-50 with different incubation periods did not increase cytotoxicity compared to the control. Overall, neither the MTS nor LDH assays resulted in evidence of cytotoxicity.

Concentrations of 200 and 250 µg/ml of PP-50 were chosen for apoptosis and morphological analysis. These concentrations were 10-fold higher than the one proven to improve cryosurvival, and were selected in order to ensure the visualisation of any morphological or apoptotic effects of PP-50 [8].

To investigate the induction of cellular apoptosis as a result of incubation with PP-50, cells treated with the polymer were evaluated with Annexin V-FITC/PI and then analysed by flow cytometry (Fig. 4). Annexin V is widely used in conjunction with PI to determine whether cells are viable, apoptotic, or necrotic through differences in plasma membrane integrity and permeability [34]. Apoptosis in PP-50 treated cells accounted for approximately 10% of the total population for both 2 and 24 hour incubations. When compared to untreated cells, PP-50 treated cells had a reduction in apoptosis of 50% and 21%, respectively. PP-50 treated cells also showed a significant reduction in necrotic cells from the control. In addition, when compared to staurosporine, an apoptosis inducer, PP-50 showed a significant decrease in apoptotic cells thus supporting its biocompatibility.

It was observed that after a 2 hour incubation, the percentage of apoptotic cells amongst untreated cells was higher than expected (around 20%). This may be explained by the use of trypsin, a protease with proteolytic activity, to detach the cells during the harvesting process, which may lead to false positives due to mechanical damage [35,36].

To further investigate the effect of PP-50, changes in cell morphology and cell detachment from the wells were also used as indicators of viability (Fig. 5). Phase contrast microscopy showed standard cytoskeletons with a regular structure and only a marginal cell detachment

in cells incubated with 250 µg/ml of PP-50 for both 2 and 24 hours. No morphological differences were seen in cells treated with PP-50 when compared to untreated cells.

PP-50 treated cells were subsequently analysed using confocal microscopy. Propidium iodide, a non-permeable dye, was used to assess cell viability as it is not taken up by living cells [34,37]. Calcein, a non-permeable hydrophilic dye which accounts for the activity of cytoplasmic esterases, was used to both stain cells capable of incorporating it into their cytoplasm and to simultaneously assess any PP-50 transport of the dye into the cytoplasm [38,39]. As shown in Fig. 6, no propidium iodide positive cells were seen in incubations with PP-50, again demonstrating that PP-50 is not cytotoxic to cells. Cells incubated with PP-50 displayed increased staining with calcein when compared to controls, hence demonstrating PP-50's ability to permeabilise cell membranes with hydrophilic molecules, as previously shown [8,28].

Transmission electron microscopy was used to investigate morphological changes in PP-50 treated cells that could have been omitted by other methods (Fig. 7). However, no difference in either morphology or size of PP-50 treated cells was found when compared to untreated cells. This is in agreement with previous methods used in this study to assess the cellular effect of PP-50.

In this work, PP-50 has been shown to have no cytotoxic effects on osteosarcoma cells, making it well suited for use in existing cell cryopreservation protocols and therapeutic applications. In addition, the complete set of protocols used to assess cell viability in the presence of PP-50 can also be used with different polymers in future studies.

6. Conclusions

In this study, the cellular effect of an amphipathic pH-responsive biopolymer was studied. PP-50 concentrations ranging from 10 to 2,000 µg/ml were shown to have no negative effect on doubling time, metabolic activity and lactate dehydrogenase release in SAOS-2 cells. PP-50 did not induce any additional apoptosis or necrosis in polymer treated cells compared to the control, highlighting a potential use in cell-based protocols for drug delivery. Incubation with PP-50 did not alter cell morphology in any way as shown by microscopy analysis, showing the safety of this polymer at the concentrations tested. Further work is needed to determine the effect of PP-50 in different cell systems, such as suspension cells or in vivo models. This study provides an important step toward the use of amphipathic biopolymers for cryopreservation and biomedical applications.

7. Acknowledgements

Mercado S. A. wishes to thank the Agency for Science and Technology Research, CONICYT (Chile), for the provision of a studentship during the tenure of which this work was conducted. The authors would like to thank Nigel Miller, Department of Pathology, Dr Jeremy Skepper, Department of Anatomy, Radu Lazar, Dr Hassan Rahmoune and Dr Krishna Mahbubani, Department of Chemical Engineering and Biotechnology, all from the University of Cambridge.

8. References

- [1] D. Hutanu, Recent Applications of Polyethylene Glycols (PEGs) and PEG Derivatives, *Mod Chem Appl.* 02 (2014) 2–7. doi:10.4172/2329-6798.1000132.
- [2] M. Hrubý, S.K. Filippov, P. Štěpánek, Smart polymers in drug delivery systems on crossroads: Which way deserves following?, *European Polymer Journal.* 65 (2015) 82–97. doi:10.1016/j.eurpolymj.2015.01.016.
- [3] L. Meng, X. Zhang, Q. Lu, Z. Fei, P.J. Dyson, Single walled carbon nanotubes as drug delivery vehicles: targeting doxorubicin to tumors, *Biomaterials.* 33 (2012) 1689–98. doi:10.1016/j.biomaterials.2011.11.004.
- [4] B. Ziemia, G. Matuszko, D. Appelhans, B. Voit, M. Bryszewska, B. Klajnert, Genotoxicity of poly(propylene imine) dendrimers, *Biopolymers.* 97 (2012) 642–648. doi:10.1002/bip.22056.
- [5] W.B. Liechty, D.R. Kryscio, B. V. Slaughter, N.A. Peppas, Polymers for Drug Delivery Systems, *Annual Review of Chemical and Biomolecular Engineering.* 1 (2010) 149–173. doi:10.1146/annurev-chembioeng-073009-100847.
- [6] M. Efentakis, S. Politis, Comparative evaluation of various structures in polymer controlled drug delivery systems and the effect of their morphology and characteristics on drug release, *European Polymer Journal.* 42 (2006) 1183–1195. doi:10.1016/j.eurpolymj.2005.11.009.
- [7] H. Vihola, A. Laukkanen, L. Valtola, H. Tenhu, J. Hirvonen, Cytotoxicity of thermosensitive polymers poly(N-isopropylacrylamide), poly(N-vinylcaprolactam) and amphiphilically modified poly(N-vinylcaprolactam), *Biomaterials.* 26 (2005) 3055–3064. doi:10.1016/j.biomaterials.2004.09.008.
- [8] D.M.C. Sharp, A. Picken, T.J. Morris, C.J. Hewitt, K. Coopman, N.K.H. Slater, Amphipathic polymer-mediated uptake of trehalose for dimethyl sulfoxide-free human cell cryopreservation, *Cryobiology.* 67 (2013) 305–311. doi:10.1016/j.cryobiol.2013.09.002.

- [9] A.L. Lynch, N.K.H. Slater, Influence of intracellular trehalose concentration and pre-freeze cell volume on the cryosurvival of rapidly frozen human erythrocytes, *Cryobiology*. 63 (2011) 26–31. doi:10.1016/j.cryobiol.2011.04.005.
- [10] S. Zhang, H. Qian, Z. Wang, J. Fan, Q. Zhou, G. Chen, et al., Preliminary study on the freeze-drying of human bone marrow-derived mesenchymal stem cells, *J Zhejiang Univ-Sci B*. 11 (2010) 889–894. doi:10.1631/jzus.B1000184.
- [11] G. Pless, I.M. Sauer, U. Rauen, Improvement of the cold storage of isolated human hepatocytes, *Cell Transplantation*. 21 (2012) 23–37. doi:10.3727/096368911X580509.
- [12] I. Ginis, B. Grinblat, M.H. Shirvan, Evaluation of Bone Marrow-Derived Mesenchymal Stem Cells After Cryopreservation and Hypothermic Storage in Clinically Safe Medium, *Tissue Engineering*. 18 (2012). doi:10.1089/ten.tec.2011.0395.
- [13] T. Chen, J.P. Acker, A. Eroglu, S. Cheley, H. Bayley, A. Fowler, et al., Beneficial effect of intracellular trehalose on the membrane integrity of dried mammalian cells, *Cryobiology*. 43 (2001) 168–181. doi:10.1006/cryo.2001.2360.
- [14] C. Polge, A.U. Smith, A.S. Parkes, Revival of spermatozoa after vitrification and dehydration at low temperatures, *Nature*. 164 (1949) 666. doi:10.1038/164666a0.
- [15] L. JE, B. MW, Prevention of freezing damage to living cells by dimethyl sulphoxide, *Nature*. (1959) 1394–1395.
- [16] E. Szurek, A. Eroglu, Comparison and avoidance of toxicity of penetrating cryoprotectants, *PloS One*. 6 (2011) e27604. doi:10.1371/journal.pone.0027604.
- [17] K. Moore, A.Q. Bonilla, Cryopreservation of Mammalian Embryos : The State of the Art, *Annual Review of Biomedical Sciences*. 8 (2006) 19–32. doi:10.5016/1806-8774.2006v8p19.
- [18] C.J. Hunt, Cryopreservation of Human Stem Cells for Clinical Application: A Review, *Transfus Med Hemother*. 38 (2011) 107–123. doi:10.1159/000326623.
- [19] H. Meyer, O. Vitavska, H. Wiczorek, Identification of an animal sucrose transporter, *Journal of Cell Science*. 124 (2011) 1984–1991. doi:10.1242/jcs.082024.
- [20] A. Eroglu, M.J. Russo, R. Bieganski, A. Fowler, S. Cheley, H. Bayley, et al., Intracellular trehalose improves the survival of cryopreserved mammalian cells, *Nature Biotechnology*. 18 (2000) 163–167. doi:10.1038/72608.
- [21] P.E.R. Tatham, M. Lindau, ATP-induced pore formation in the plasma membrane of rat peritoneal mast cells, *The Journal of General Physiology*. 95 (1990) 459–476. doi:10.1085/jgp.95.3.459.
- [22] G.D. Elliott, X.-H. Liu, J.L. Cusick, M. Menze, J. Vincent, T. Witt, et al., Trehalose uptake through P2X7 purinergic channels provides dehydration protection, *Cryobiology*. 52 (2006) 114–127. doi:10.1016/j.cryobiol.2005.10.009.

- [23] E. Adinolfi, C. Pizzirani, M. Idzko, E. Panther, J. Norgauer, F. Di Virgilio, et al., P2X(7) receptor: Death or life?, *Purinergic Signalling*. 1 (2005) 219–227. doi:10.1007/s11302-005-6322-x.
- [24] A.L. Lynch, R. Chen, P.J. Dominowski, E.Y. Shalaev, R.J. Yancey, N.K.H. Slater, Biopolymer mediated trehalose uptake for enhanced erythrocyte cryosurvival, *Biomaterials*. 31 (2010) 6096–103. doi:10.1016/j.biomaterials.2010.04.020.
- [25] P.S. Stayton, A.S. Hoffman, N. Murthy, C. Lackey, C. Cheung, P. Tan, et al., Molecular engineering of proteins and polymers for targeting and intracellular delivery of therapeutics, *Journal of Controlled Release*. 65 (2000) 203–220. doi:10.1016/S0168-3659(99)00236-9.
- [26] J.C. Chung, D.J. Gross, J.L. Thomas, D.A. Tirrell, L.R. Opsahl-Ong, pH-Sensitive, Cation-Selective Channels Formed by a Simple Synthetic Polyelectrolyte in Artificial Bilayer Membranes, *Macromolecules*. 29 (1996) 4636–4641. doi:10.1021/ma9600522.
- [27] J.L. Thomas, S.W. Barton, D.A. Tirrell, Membrane solubilization by a hydrophobic polyelectrolyte: surface activity and membrane binding, *Biophysical Journal*. 67 (1994) 1101–1106. doi:10.1016/S0006-3495(94)80575-2.
- [28] A.L. Lynch, R. Chen, N.K.H. Slater, pH-responsive polymers for trehalose loading and desiccation protection of human red blood cells, *Biomaterials*. 32 (2011) 4443–4449. doi:10.1016/j.biomaterials.2011.02.062.
- [29] V. Katsares, A. Petsa, A. Felesakis, Z. Papanicolaou, E. Nikolaidou, S. Gargani, et al., A Rapid and Accurate Method for the Stem Cell Viability Evaluation: The Case of the Thawed Umbilical Cord Blood, *Laboratory Medicine*. 40 (2009) 557–560. doi:10.1309/LMLE8BVHYWCT82CL.
- [30] A. Tunnacliffe, J. Lapinski, Anhydrobiotic engineering, *Nature Biotechnology*. 18 (2000) 473. doi:10.1038/75237.
- [31] V.G. Almeida, M.C.X. Pinto, F.A.G. Moura, Trypan blue exclusion assay by flow cytometry, *Brazilian Journal of Medical and Biological Research*. 47 (2014) 307–315. doi:10.1590/1414-431X20143437.
- [32] D. Lobner, Comparison of the LDH and MTT assays for quantifying cell death: validity for neuronal apoptosis?, *Journal of Neuroscience Methods*. 96 (2000) 147–152. doi:10.1016/S0165-0270(99)00193-4.
- [33] D.B. Mitchell, K.S. Santone, D. Acosta, Evaluation of cytotoxicity in cultured cells by enzyme leakage, *Journal of Tissue Culture Methods*. 6 (1981) 113–116. doi:10.1007/BF02082861.
- [34] A.M. Rieger, K.L. Nelson, J.D. Konowalchuk, D.R. Barreda, Modified annexin V/propidium iodide apoptosis assay for accurate assessment of cell death, *Journal of Visualized Experiments*. (2011) 37–40. doi:10.3791/2597.

- [35] A. Bundscherer, M. Malsy, R. Lange, P. Hofmann, T. Metterlein, B.M. Graf, et al., Cell Harvesting Method Influences Results of Apoptosis Analysis by Annexin V Staining, *Anticancer Research*. 33 (2013) 3201–3204. doi:33/8/3201.
- [36] H. Huang, H. Hsing, T. Lai, Y. Chen, T. Lee, H. Chan, et al., Trypsin-induced proteome alteration during cell subculture in mammalian cells, *Journal of Biomedical Science*. 17 (2010) 36. doi:10.1186/1423-0127-17-36.
- [37] J. Fried, A.G. Perez, B.D. Clarkson, Flow cytometry analysis of cell cycle distributions using propidium iodide, *The Journal of Cell Biology*. 71 (1976) 172–181.
- [38] R. Chen, M.E. Eccleston, Z. Yue, N.K.H. Slater, Synthesis and pH-responsive properties of pseudo-peptides containing hydrophobic amino acid grafts, *Journal of Materials Chemistry*. 19 (2009) 4217–4224. doi:10.1039/b902822f.
- [39] R. Chen, S. Khormae, M.E. Eccleston, N.K.H. Slater, The role of hydrophobic amino acid grafts in the enhancement of membrane-disruptive activity of pH-responsive pseudo-peptides, *Biomaterials*. 30 (2009) 1954–1961. doi:10.1016/j.biomaterials.2008.12.036.

Figure captions

Figure 1: Cellular growth curves (solid lines) and viabilities (dashed lines) of SAOS-2 cells in the absence or presence of PP-50. Measurements were determined by the trypan blue dye exclusion method. Data were derived from three replicates. Error bars represent the standard error.

Figure 2: Metabolic activity of SAOS-2 cells after incubation for 2, 24 and 48 hours with various concentrations of PP-50. Data were normalised to cells incubated in the absence of PP-50 for the same incubation time. Data were derived from three replicates. Error bars represent standard error.

Figure 3: Lactate dehydrogenase released by SAOS-2 cells after incubation for 2, 24 and 48 hours with various concentrations of PP-50. Untreated cells were grown and analysed in the absence of PP-50. Data were derived from three replicates. Error bars represent standard error.

Figure 4: Percentage of apoptotic and necrotic SAOS-2 cells after incubation with PP-50. Black bars represent apoptotic cells and grey bars represent necrotic cells. A) Incubation for 2 hours with PP-50 (250 µg/ml). B) Incubation for 24 hours with PP-50 (250 µg/ml). Apoptosis and necrosis were determined by flow cytometry using Annexin V- FITC/PI. Cells positive only for Annexin V were considered to be apoptotic. Cells positive for both Annexin

V and PI were considered to be necrotic. Data were derived from three replicates. Error bars represent standard errors. * denotes significant difference compared to untreated cells or as indicated in the figure ($p < 0.05$).

Figure 5: Effect of PP-50 on SAOS-2 cell morphology as determined by phase contrast microscopy. A) Control cells incubated in the absence of PP-50. B) Cell incubation for 2 hours with PP-50 (250 $\mu\text{g/ml}$). C) Cell incubation for 24 hours with PP-50 (250 $\mu\text{g/ml}$). D) Cell incubation with 5 μM of staurosporine for 4 hours. Morphological changes were examined and photographed using a phase contrast microscope. Data are representative of a minimum of three separate experiments.

Figure 6: Confocal microscopy images of SAOS-2 cells fixed with 4% paraformaldehyde or incubated in the absence and presence of PP-50 (200 $\mu\text{g/ml}$) for 24 hours. Cells were first stained with 2 mM calcein (green fluorescence) and subsequently with 5 $\mu\text{g/ml}$ propidium iodide (red fluorescence) and 5 $\mu\text{g/ml}$ Hoechst H33342 (blue fluorescence). Data are representative of a minimum of three separate experiments.

Figure 7: Effect of PP-50 on SAOS-2 cell morphology as determined by transmission electron microscopy. A) Control cells incubated in the absence of PP-50. B) Cell incubation for 2 hours with PP-50 (250 $\mu\text{g/ml}$). C) Cell incubation for 24 hours with PP-50 (250 $\mu\text{g/ml}$). Data are representative of a minimum of three separate experiments. Scale bars represent 2 μm .

Figure 1

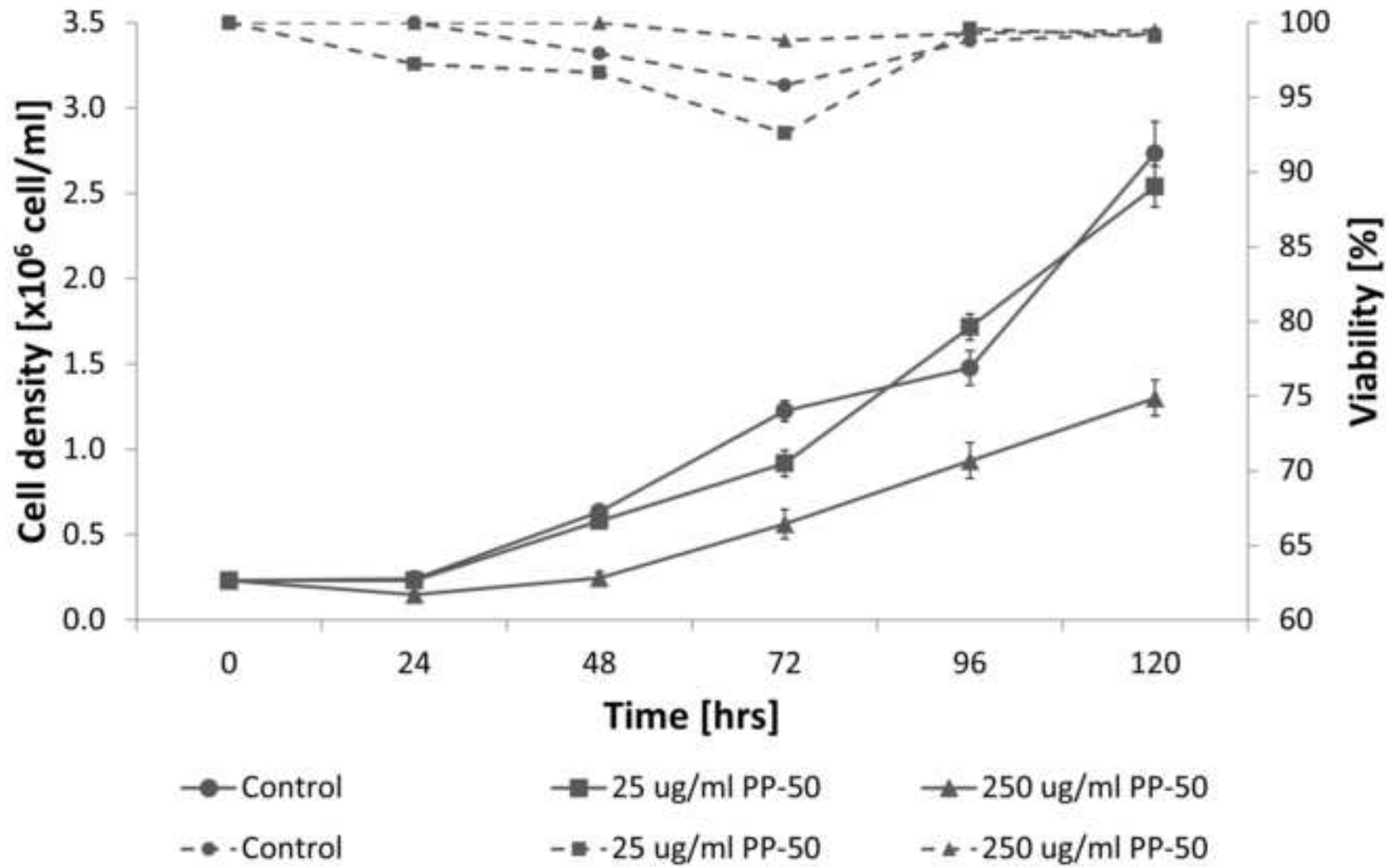


Figure 2

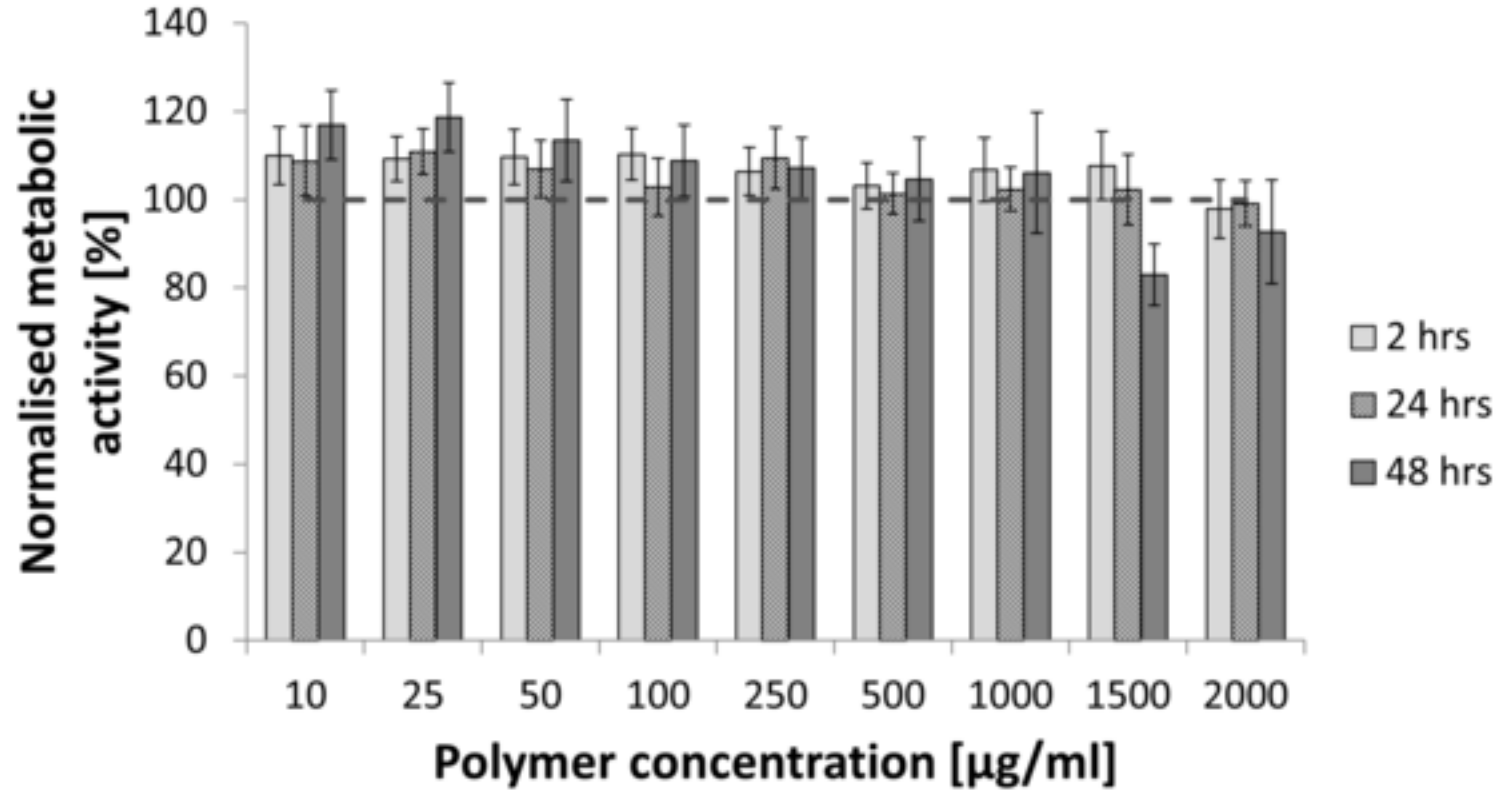


Figure 3

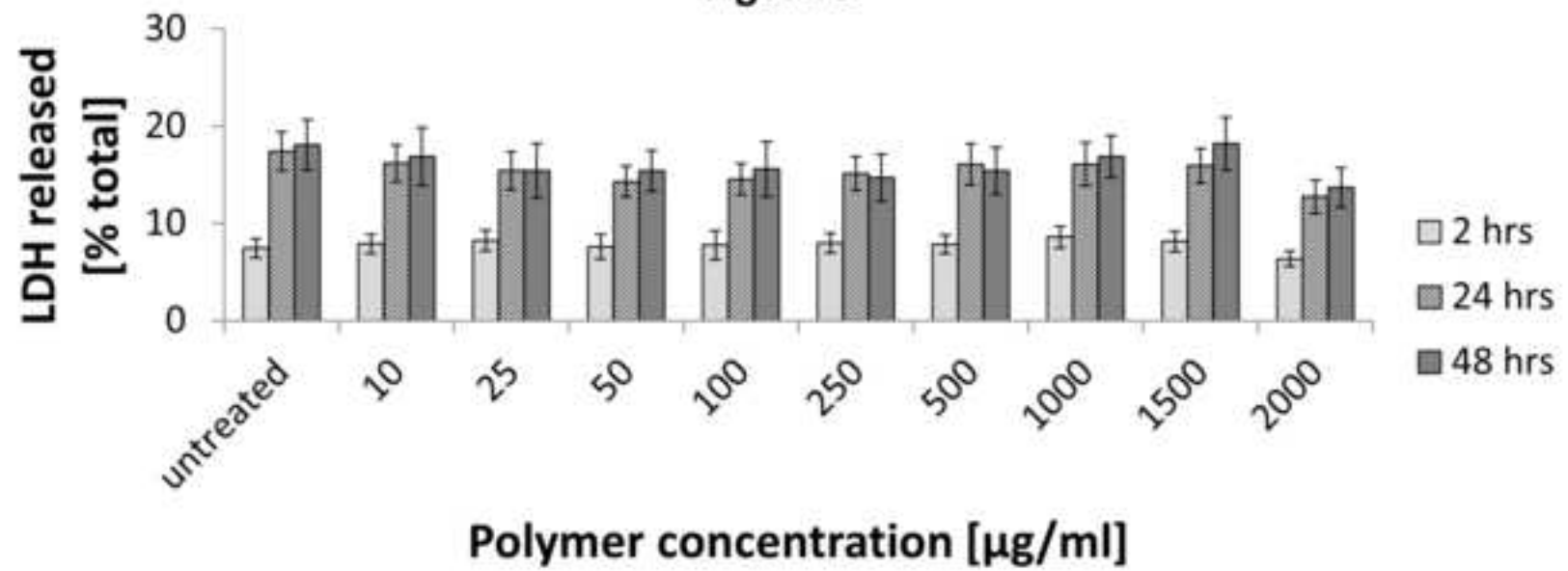


Figure 4

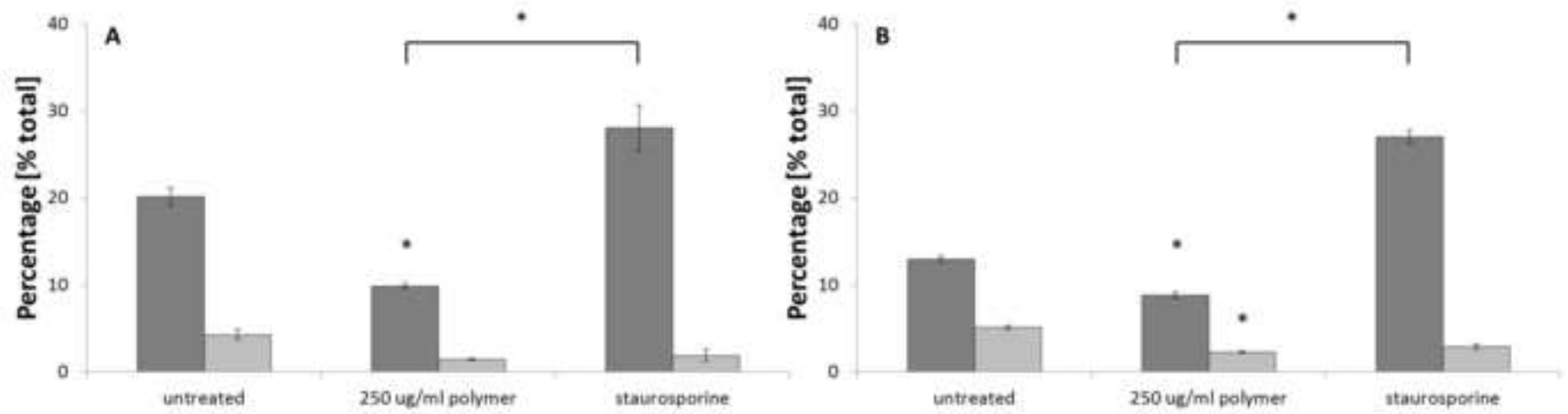


Figure 5

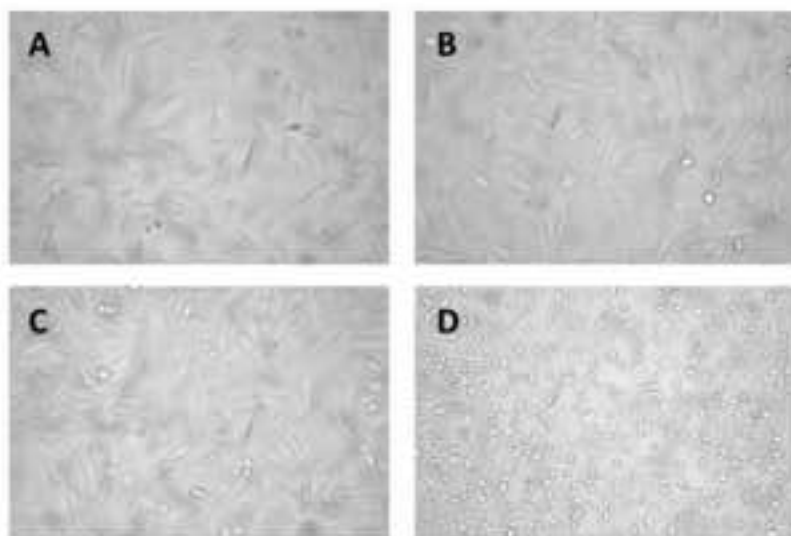


Figure 6

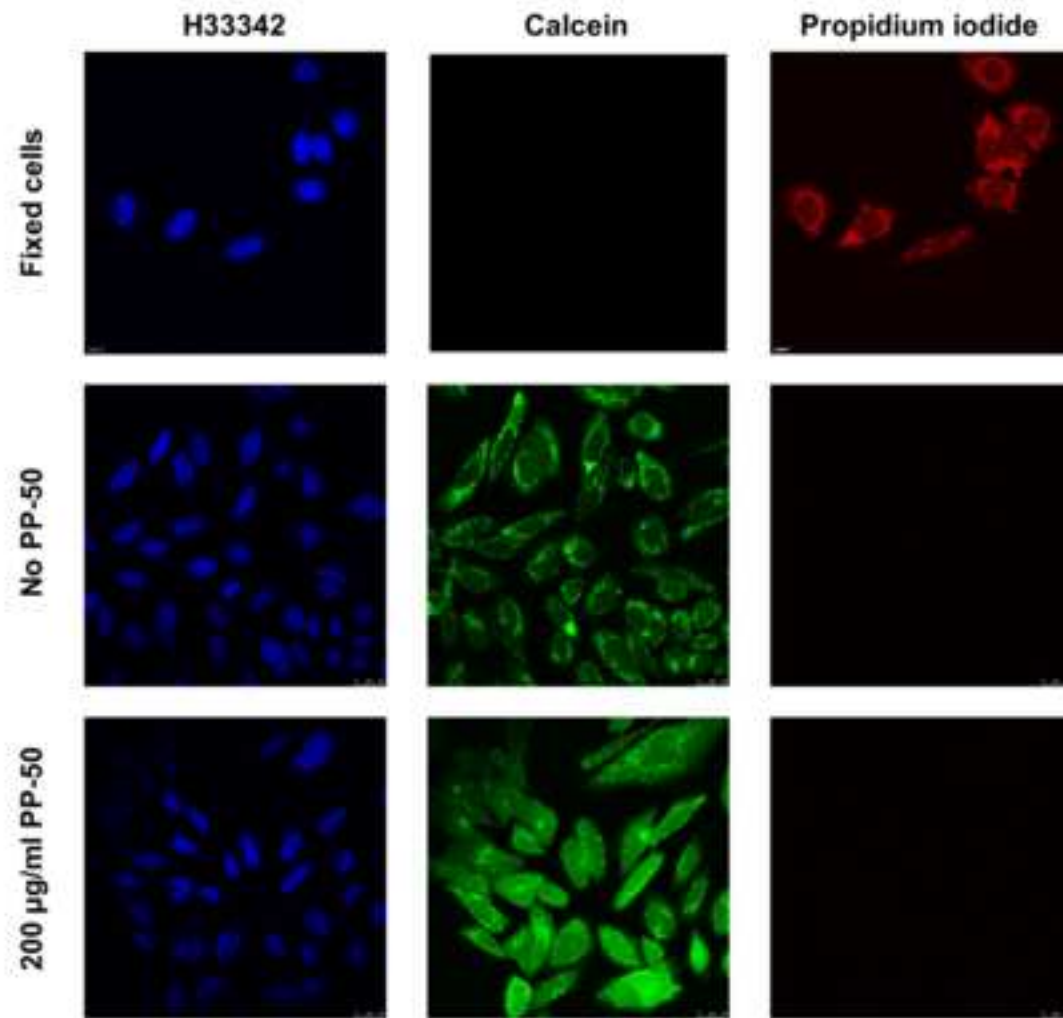


Figure 7

